Trends in Biotechnology

CellPress

Review

Pushing the rheological and mechanical boundaries of extrusion-based 3D bioprinting

Liliang Ouyang [1,2,3,4,*,@]

3D bioprinting has long been subjected to trade-offs between physicochemical and biological outcomes. The resulting material properties of the initial bioinks and final printing products usually lie within a moderate range, which limits the application of bioprinting and its products. Recent progress in bioinks and bioprinting techniques has significantly expanded the window of material properties. In this review, I define two bioprinting windows to clarify the trade-offs between physical chemistry and biology and provide a comprehensive overview of recent advances that have pushed the rheological boundaries of bioinks and mechanical boundaries of bioprints, focusing on unusual material properties. I illustrate this with recent examples, consolidate the existing strategies into well-defined categories, highlight the prominent trends, and provide perspectives on additional boundaries.

Highlights

Two bioprinting windows are defined based on the long-existing concept of biofabrication window to sufficiently describe the complete 3D bioprinting process, covering the structural printing and the subsequent biological cultivation.

The poorly fulfilled requirement for super-soft bioprints (with modulus of the order of ≤1 kPa) that favor the culture of cells with a soft tissue origin has significantly driven the efforts on the expansion of bioprinting windows.

Innovative crosslinking strategies have enabled the printing of liquid-like (or low-viscosity) bioinks, and the fabrication of innovative gel-phase formulations has advanced the bioprinting of solid-like bioinks.

A fundamental principle for printing exceptionally soft hydrogels is to incorporate sacrificial materials, whereas printing stiff hydrogels mainly relies on the inclusion of mechanical reinforcers, both of which span from the mesoscale to the nanoscale range.

Additional boundaries toward cell-rich bioinks and mechanically dynamic bioprints contribute toward the biomimicry of engineering functional tissues.

The trade-off between physical chemistry and biology: a fundamental consideration for 3D bioprinting

In the past decade, **3D bioprinting** (see Glossary) has advanced as a powerful technology for numerous biomedical applications, including tissue engineering, disease modeling, and drug testing [1]. 3D bioprinting can engineer customized living constructs with many degrees of freedom through the application of an **additive manufacturing** principle and using living cells as raw materials. Despite considerable progress, there remains an enduring challenge for bioprinting: a trade-off between physicochemical and biological outcomes. In other words, 3D printing is often expected to yield a physically robust structure, but the embedded cells in **bioinks** usually require mild processing conditions and a relatively soft matrix environment. Malda and colleagues [2] introduced the concept of 'biofabrication window' to describe the trade-off for general biofabrication and referred to it as 'the range of material properties suitable both for printability with high shape fidelity and for the support of cell function' [3]. Indeed, the material properties usually fit into a moderate range, resulting in a narrow biofabrication window. Expanding the window will significantly contribute toward bioink development and increase the capacities of 3D bioprinting.

Recent advances in bioprinting have pushed the boundaries of material properties to a considerably wider range. For example, solid-phase bioinks have been developed beyond the typical viscous solution state [4,5]. Indeed, bioink properties have attracted considerable attention as they are crucial for the bioprinting process in which the ink containing live cells undergoes extrusion. However, the physicochemical properties of bioinks do not necessarily represent the properties of the printed constructs, which provide a foundation for cells to grow over time. Thus, in this review, I define two separate bioprinting windows specifically for the 3D bioprinting process associated with two different stages: printing and cultivation (Figure 1, Key figure). I discuss the most recent advances that have expanded the corresponding windows for **extrusion-based bioprinting**, and provide my perspectives on future trends. Based on the recently reported innovative forms of bioinks and bioprinting and the exhibited unusual properties,

[1]Department of Mechanical Engineering, Tsinghua University, Beijing 100084, China
[2]Biomanufacturing and Rapid Forming Technology Key Laboratory of Beijing, Tsinghua University, Beijing 100084, China
[3]"Biomanufacturing and Engineering Living Systems" Innovation International Talents Base (111 Base), Tsinghua University, Beijing 100084, China
[4]Lab website: https://llouyang.com/

this review aims to highlight the boundaries of extrusion-based 3D bioprinting. The existing reviews have covered the general strategies for the development of bioinks and bioprinting technologies [3,6], while others have focused on particular material properties, such as mechanical reinforcement [7]. There needs one timely review that updates the concept and content of bioprinting windows, specifically highlighting the bioprinting of ultrasoft constructs, which has been rarely discussed before. Together, this review is intended to inspire researchers who are studying bioinks and 3D bioprinting for biomedical applications.

*Correspondence:
ouy@tsinghua.edu.cn (L. Ouyang).
@Twitter: @liliangouyang

Bioprinting windows: from the rheology of bioinks to the mechanics of bioprints

Bioprinting window: rheology of bioinks

For extrusion-based 3D bioprinting technology, bioinks are typically required to possess suitable rheological properties to maintain the shape of extruded filaments and thus achieve a desirable

Key figure

Schematic of two bioprinting windows

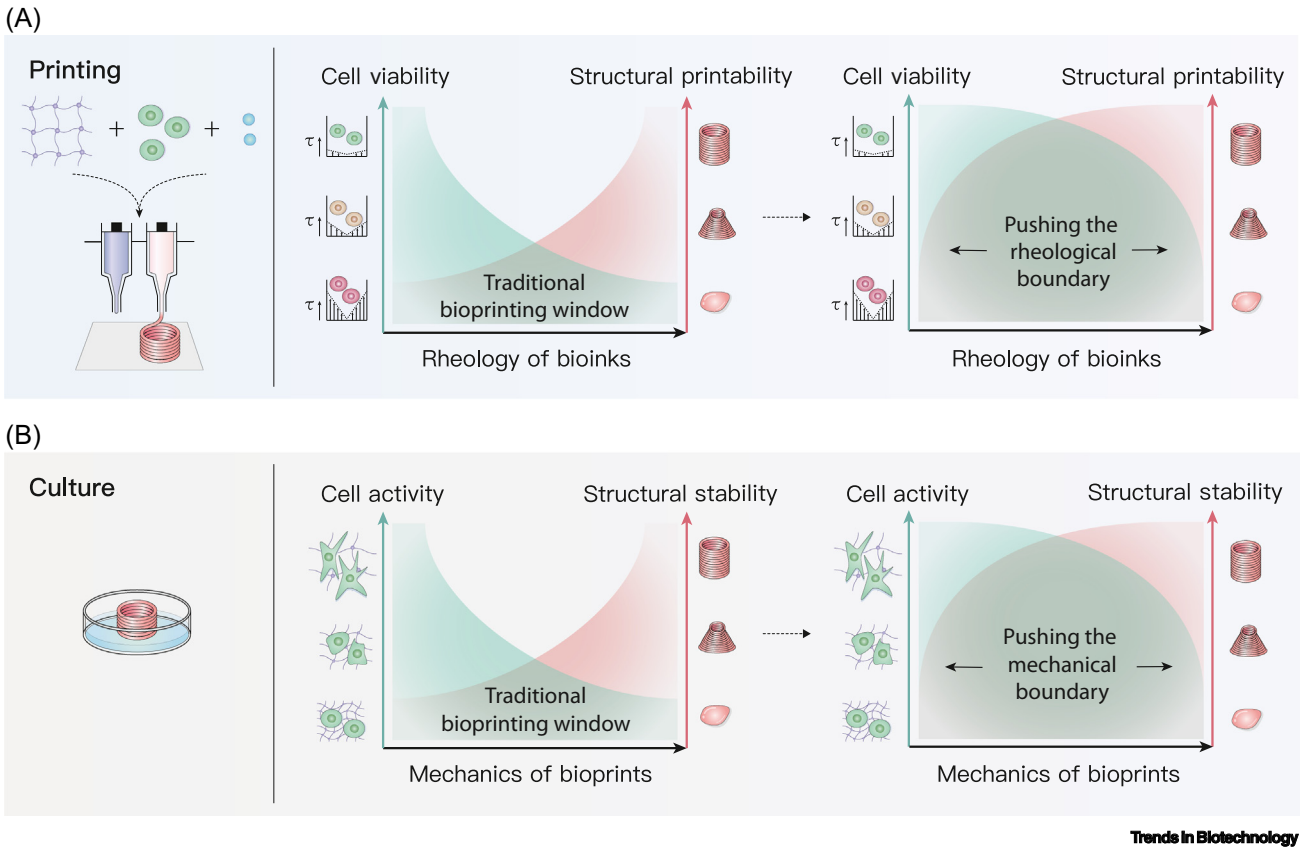

Figure 1.

For a Figure360 author presentation of Figure 1, see the figure legend at https://doi.org/10.1016/j.tibtech.2022.01.001.

(A) The bioprinting window during printing refers to the rheology of bioinks, considering cell viability and structural printability. (B) The bioprinting window during cultivation (i.e., after printing) relates to the mechanics of bioprints, taking cell activity and structural stability into consideration. Pushing the boundaries of corresponding characteristics expands the windows and eases the trade-offs between physicochemical and biological outcomes.

printability. Printability is a vague concept but has been characterized and appropriately quantified in recent years. For example, a printability value (Pr) was introduced to characterize the structural outcomes and differentiate the gelation status of bioinks during printing [8]. Based on the strong relationship between bioink **rheology** and structure fidelity, other studies have used rheological characteristics to govern and predict printability. **Viscosity** is probably the most well-known parameter, and it is commonly believed that a relatively high viscosity contributes toward shape maintenance and structural fidelity [9]. **Yield stress** is another important characteristic and usually correlates with shear-thinning and self-healing properties, which are desirable viscoelastic characteristics for extrusion-based printing. Applied shear stress exceeding the yield stress increases flowability, whereas the elimination of the shear stress would result in a recovery of the modulus [10]. Nevertheless, these rheological requirements of bioinks might not be applicable to other bioprinting technologies such as vat polymerization-based bioprinting.

The inclusion of living cells in the manufacturing process makes bioprinting unique. The importance of protecting cells has long been realized, and the shear force applied to cells during extrusion through a narrow needle is believed to be a major cause of cell damage [11,12]. For example, an apparent decrease in cell viability was observed with an increase in the maximum shear stress in the printer needle. To achieve a cell viability of more than 80% for the bioprinting of embryonic stem cells, the maximum shear stress should be maintained below ~100 Pa [8]. In another example, Chen and colleagues [13] found that the extensional stress in the geometrically contractive area could also induce cell damage. Nevertheless, it is considered good practice to control the flow-induced stress on cells to ensure a high cell survival rate after extrusion, while such stress normally exhibits a positive correlation with viscosity. It should be noted that the inclusion of cells in the bioinks would affect the rheological outcomes, which, however, has been often overlooked. Together, structural printability and cell viability during printing have nearly opposite requirements for bioink rheology, which results in a moderate parameter range for bioprinting (Figure 1A).

Bioprinting window: mechanics of bioprints

The cultivation of bioprints over time is significant, leading to another bioprinting window representing the mechanical properties of bioprints during biological cultivation *in vitro*. This window is often overlooked and mixed with that of bioink rheology. However, cells that survive the extrusion process may not necessarily grow well later on. Similarly, well-printed 3D constructs at the printing stage may be further affected regarding the shape fidelity owing to cell-mediated effects [14] and the unexpected effects caused by the physiological conditions *in vitro* (normally immersed in a suitable culture medium in an incubator at 37°C and 5% CO_2). **Hydrogels**, which are nearly the only type of cell carrier biomaterial in bioprinting, are generally soft, as the majority of their content is water. It is believed that stiff or strong hydrogels are beneficial for maintaining structural fidelity during cultivation [7,15]. The current bioprinted hydrogels that exhibit high shape fidelity during culture usually possess a stiffness of magnitude of 10 kPa or higher [16], regardless of the rheology of the original bioink.

In nature, native tissues possess highly varied mechanical properties depending on their origin. For example, the modulus of bone tissue is in the range of 10^6–10^7 kPa, while that of brain tissue only ranges from 1 kPa to 3 kPa [17]. In the context of 3D cell culture, the engineered **extracellular matrix** (ECM) does not necessarily need to fully match the mechanical properties of the matured native tissue, considering the secretion and remodeling of matrices during tissue formation. However, it is still crucial to provide a suitable initial mechanical microenvironment to initiate the appropriate cellular processes. A common finding is that excessively stiff hydrogels significantly hinder the proliferation and migration of embedded cells [18]. Even engineering of skeletal tissues

Glossary

3D bioprinting: the use of 3D printing technologies to fabricate biological models.
Additive manufacturing: a process used to create a 3D object by layering materials one by one based on a digital model; it is a terminology changeable with 3D printing.
Bioinks: a formulation of cells that is suitable to be processed by an automated biofabrication technology.
Crosslinking: a process that generates a physical or chemical bond that links one polymer chain with another.
Decellularized ECM: ECM isolated from native tissues by chemically or physically removing the inhibiting cells.
Double network hydrogel: a hydrogel containing two types of networks with contrasting properties.
Extracellular matrix (ECM): a 3D network of extracellular macromolecules and minerals that provide structural and biochemical support to the surrounding cells.
Extrusion-based bioprinting: a type of bioprinting that applies an extrusion force to drive the flow of bioinks, which are expected to form filament-shaped building blocks for layered deposition.
Hydrogel: a 3D crosslinked network of hydrophilic polymers dissolved in water with the ability to hold a large amount of water.
Melt electrowriting: a fabrication technique derived from electrospinning that allows for the defined placing of microfibers.
Printability: the ability of a bioink and the bioprinting process to deliver a structure based on a computer-aided design model.
Rheology: a branch of physics that studies the deformation and flow of matter, both solids and liquids.
Viscosity: measure of a fluid's resistance to deformation at a given shear rate.
Yield stress: the stress corresponding to the yield point at which the material begins to deform plastically in response to an external force.

might require a relatively soft microenvironment to initiate tissue formation [19]. Together, the requirements from structural stability and cell activity have typically led to a traditional bioprinting window in which bioprints exhibit moderate strength (Figure 1B).

Pushing the rheological boundaries of bioinks

Bioprinting liquid-like (low-viscosity) bioinks

A bioink is usually a formulation of cells dispersed in hydrogel precursor solutions, which could be prepared from different types of polymers, including protein, saccharide, and synthetic polymers. The **crosslinking** of these polymers plays a critical role in the 3D bioprinting process, particularly in the processing of liquid-like bioinks. An *in situ* crosslinking strategy has been developed for the direct bioprinting of nonviscous photo-crosslinkable hydrogels [20] [Figure 2A(i)]. By incorporating a photo-permeable needle and introducing light *in situ*, the liquid-like formulations were partially crosslinked simultaneously to generate a smooth filament, and they maintained a high cell viability (~90%) after printing. In contrast, the pre-photo-crosslinking induced nonuniform filament shape and extrusion force, together with reduced cell viability (~40%) probably due to the high shear stress [20]. The *in situ* crosslinking strategy is highly generalizable to a series of photo-crosslinkable hydrogels, all in a low-viscosity range (<15 mPa·s). This strategy has also been adapted to the coaxial bioprinting process, where a shell flow is used to smoothen the flow of the inner photo-crosslinkable bioink with light introduced *in situ* [21]. Using a similar approach, a recent study claimed that 1–6 wt% gelatin methacryloyl (GelMA) could be printed [22], although

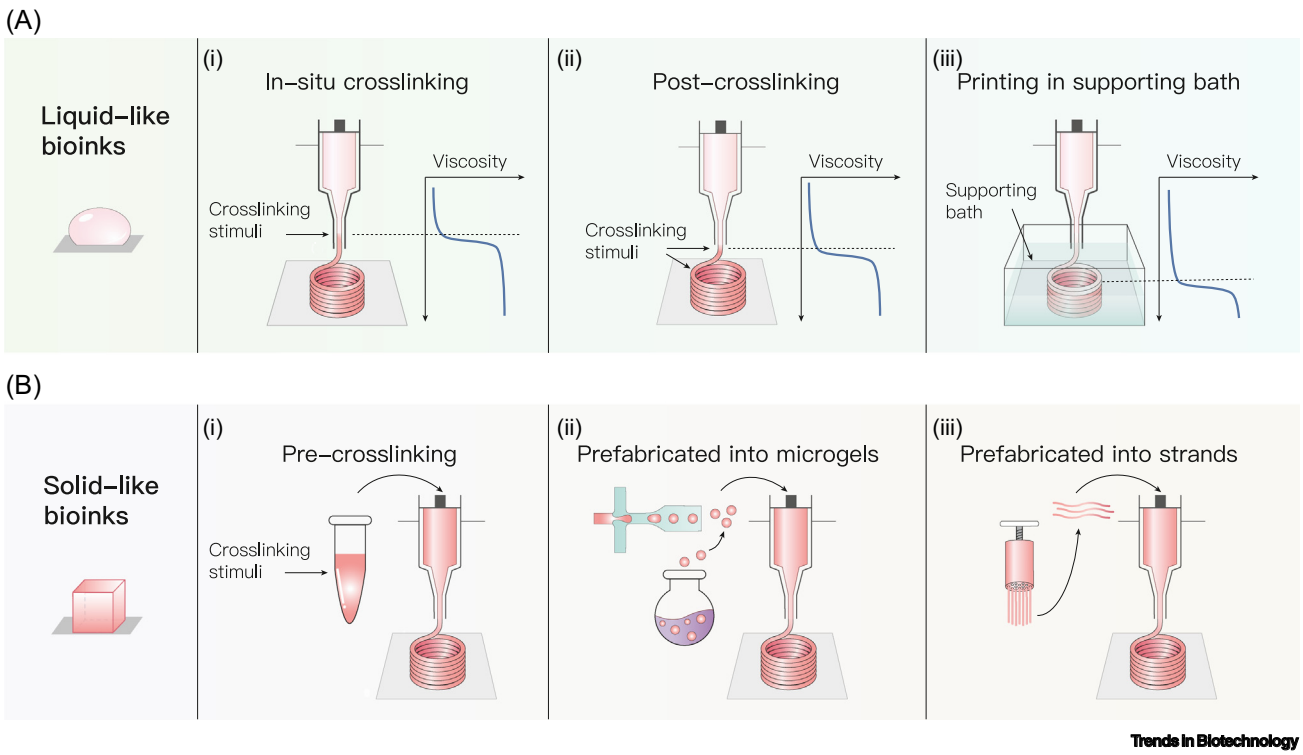

Figure 2. Representative strategies for pushing the rheological boundaries of bioinks. (A) For the printing of liquid-like (low-viscosity) bioinks, the position and timing of crosslinking stimuli are critical. (i) *In situ* crosslinking applies crosslinking stimuli at the needle site to shape and stabilize the bioinks into filaments prior to leaving the nozzle. (ii) Post-crosslinking relies on rapid crosslinking mechanisms using crosslinking stimuli immediately after the ink extrusion. (iii) Printing into a suspension bath takes advantage of the support from the surrounding bath materials, which could also be incorporated with crosslinking stimuli to induce crosslinking. (B) For the printing of solid-like (gel-phase) bioinks, it is crucial to protect embedded cells from the shearing process while maintaining structural printability. (i) Suitable pre-crosslinking enhances the rheological properties for shape fidelity and can potentially safeguard cells. (ii, iii) An emerging methodology to develop solid-like bioinks is prefabricating cell-laden formulations into varied forms of modular microgels (e.g., spherical and fibrous), which could be packed to deliver desirable rheological properties for printing.

the ability to build up a 3D hydrogel construct was to be further investigated. The *in situ* photocrosslinking could also be used to induce an aligned structure for muscle tissue engineering [23]. Some studies mediated the printability of initially liquid-like formulations via crosslinking before extrusion [24], which suited more in the typical strategy of viscosity enhancement.

It is convenient to perform feasible *in situ* or post-crosslinking [Figure 2A(ii)] for the bioprinting of low-viscosity alginate bioink owing to its fast gelation mechanism with divalent cations. A coaxial needle was used to deliver cell-laden alginate to the core and calcium ions (Ca^{2+}) to the shell, triggering rapid crosslinking at the end of the needle [25]. Using this approach, a 4% alginate and 4.5% GelMA mixture with low viscosity (80 mPa·s at a shear rate of 10 s^{-1}) could be printed into 3D constructs with excellent shape fidelity, while the embedded human umbilical vein endothelial cells possessed considerable viability (~75%) throughout the construct. Technically, this approach could be used to print a series of alginate-based bioinks in the low viscosity range [26]. Another paradigm for printing low-viscosity alginate is printing into a crosslinking bath. For example, an alginate-based composite bioink with relatively low viscosity [442 mPa·s at a shear rate of 10 s^{-1}, equal to 1–2 Pa of storage modulus (G')] was printed into Ca^{2+} solution for the 3D culture of Schwann cells [27]. An early study conducted by He and colleagues [28] showed the printing of perfusable constructs into a Ca^{2+} bath using a coaxial nozzle (alginate bioinks in the shell, Ca^{2+} in the core), combining *in situ* and post-crosslinking. These strategies rely heavily on a rapid crosslinking mechanism (proper gelation should occur within milliseconds), whereas many hydrogels are formed over a prolonged period depending on the crosslinking mechanism and stimuli [29,80].

Bioprinting in a suspension bath has emerged as a promising technique to enhance the capability of conventional extrusion-based bioprinting [30] [Figure 2A(iii)]. Feinberg and colleagues [31] advanced the biofabrication of nonmodified collagen, an important ECM component that usually undergoes slow gelation under physiological conditions, by printing it in a granular microgel bath that physically supports the bioink and chemically neutralizes the pH to trigger crosslinking. It was found that collagen (10–20 mg ml^{-1}) could be printed into sophisticated 3D constructs with an excellent shape fidelity. In an early study conducted by the same group [32], alginate bioink with low viscosity [G′ < loss modulus (G″) < 1 Pa at a frequency of 1 Hz] could also be printed into a microgel bath containing Ca^{2+}, yielding 3D biomimetic constructs that were challenging to fabricate on a flat substrate. Despite this progress, it is yet to be further investigated how a supporting batch could advance the bioprinting of low-viscosity bioinks with other crosslinking kinetics and to understand the underlying mechanisms.

Bioprinting solid-like (gel-phase) bioinks

Another challenge in expanding the bioprinting window involves the ability to process solid-like or gel-phase bioinks while maintaining a considerable cell survival rate. Heilshorn and colleagues [33] prepared a gel-phase alginate-protein bioink based on peptide–peptide interactions by adapting the pre-crosslinking methodology [Figure 2B(i)], which resulted in a weak hydrogel (G′ ≈ 20 Pa) with rapid shear-thinning and self-healing behavior. They found that this gel-phase bioink significantly reduced the ratio of damaged cells (<5%) compared with its plain alginate counterpart (20–40%). Despite this attractive finding, there are many examples showing a reduced cell viability from pre-crosslinking or viscosity enhancement, and controlling the degree of crosslinking or gelation of bioinks to protect the embedded cells might be challenging [20].

Recently, a new form of bioink composed of modular microgels has significantly advanced solid-like bioinks [Figure 2B(ii)]. Burdick and colleagues [4] used a fluid-focusing microfluidic device to generate microgels (diameter ~100 μm) and prepared a 'jammed' microgel formulation via vacuum filtration. The jammed formulation behaved like an elastic hydrogel at low strains and underwent a rapid,

reversible transition to a fluid state upon the application of large strains, likely due to the disrupted contacts between microgels. The authors demonstrated the printing of jammed inks composed of photo-crosslinkable hyaluronic acid, polyethylene glycol (PEG), and thermosensitive agarose. Interestingly, the cells embedded in the microgels showed a considerable cell viability of about 70%. In another example, Alsberg and colleagues [34] printed cell-laden dual-crosslinked microgels (~200 μm) composed of oxidized and methacrylated alginate into a supporting granular gel bath. They demonstrated that such cellularized microgels could be successfully cryopreserved for long-term storage (1 month) with considerable cell viability after thawing. It should be noted that a post-crosslinking is usually needed to further link the microgels and thus stabilize the printed constructs. In other examples, microgels were used as scaffold component and mixed with a continuous phase of cell-laden solution [35,36]. Efforts have also been made devoted toward better understanding the mechanism of printing microgel bioinks using computational or experimental approaches [37,38]. Recently, Gaharwar and colleagues [38] systematically investigated the mechanisms of hydrogel microgel jamming within printing nozzles and revealed the effects of printing apparatus and microgel properties on the bioprinting outcomes.

Instead of using rounded microgels, Zenobi-Wong and colleagues [5] developed a solid-like bioink based on entangled hydrogel microstrands [Figure 2B(iii)]. They deconstructed the bulk hydrogels into microstrands by sizing through a grid with apertures of 40–100 μm. The moldable microstrands could form a porous, entangled structure that was stable in an aqueous medium without further crosslinking. This new type of formulation was readily suitable for extrusion printing, where cells can be placed inside or outside the hydrogel phase with more than 90% viability, and C2C12 cells are guided to form oriented myotubes. This microstrand bioink allows for anisotropic filament formation, unlike its microgel (rounded shape) counterpart, but possesses a significantly lower void fraction (2–8%), likely due to the difficulty of isolating single microstrands in the current paradigm. Indeed, it is desirable to engineer controllable porosity in the printed filament for better mass transfer and cell infiltration. However, the jammed microgel bioink system could only yield a void fraction of 12–29% even when using varied microgel sizes. Thus, Heilshorn and colleagues [39] proposed a hybrid jammed ink composed of sacrificial gelatin and chemically crosslinked GelMA microgels. Maintaining considerable printability, the bioink would yield a void fraction of 20–57% depending on the composite ratio of the two microgels.

Pushing the mechanical boundaries of bioprints

Bioprinting soft constructs: mimicking tissues of soft origin

Direct printing of super-soft constructs in air involves the risk of structural collapse. Researchers [40] used a cryogenic 3D printing method to produce stable and soft 3D constructs (0.49 ± 0.04 kPa stress at 30% compressive strain) by introducing a freezing process to the hydrogel inks. Theoretically, this approach could achieve soft constructs owing to the temporal phase change, but its effectiveness with direct cell printing remains to be investigated. Another facile methodology is to use a sacrificial scaffold to temporally support bioprints. This can be achieved by casting a soft matrix into a premade sacrificial scaffold [41,42] or by simultaneously printing cell-laden bioinks with scaffold ink [43] [Figure 3A(i)]; the latter allows for better control over component heterogeneity and geometrical complexity. For instance, sacrificial gelatin ink and matrix GelMA ink can be printed complementarily into a void-free construct to minimize hydrogel collapse [43]. A soft and porous GelMA construct could be achieved by removing the gelatin under physiological conditions. By embedding endothelial cells in the sacrificial gelatin phase, 2D biomimetic branched [44] or 3D interconnected lattice [43] vascular networks could be achieved without the need for post cell seeding. Suspension bioprinting appears to be a promising approach for the fabrication of soft prints because of the natural support from the suspension bath [Figure 3A(i)]. Angelini and colleagues [45] achieved a fine printed structure with 1.9 mg ml^{-1}

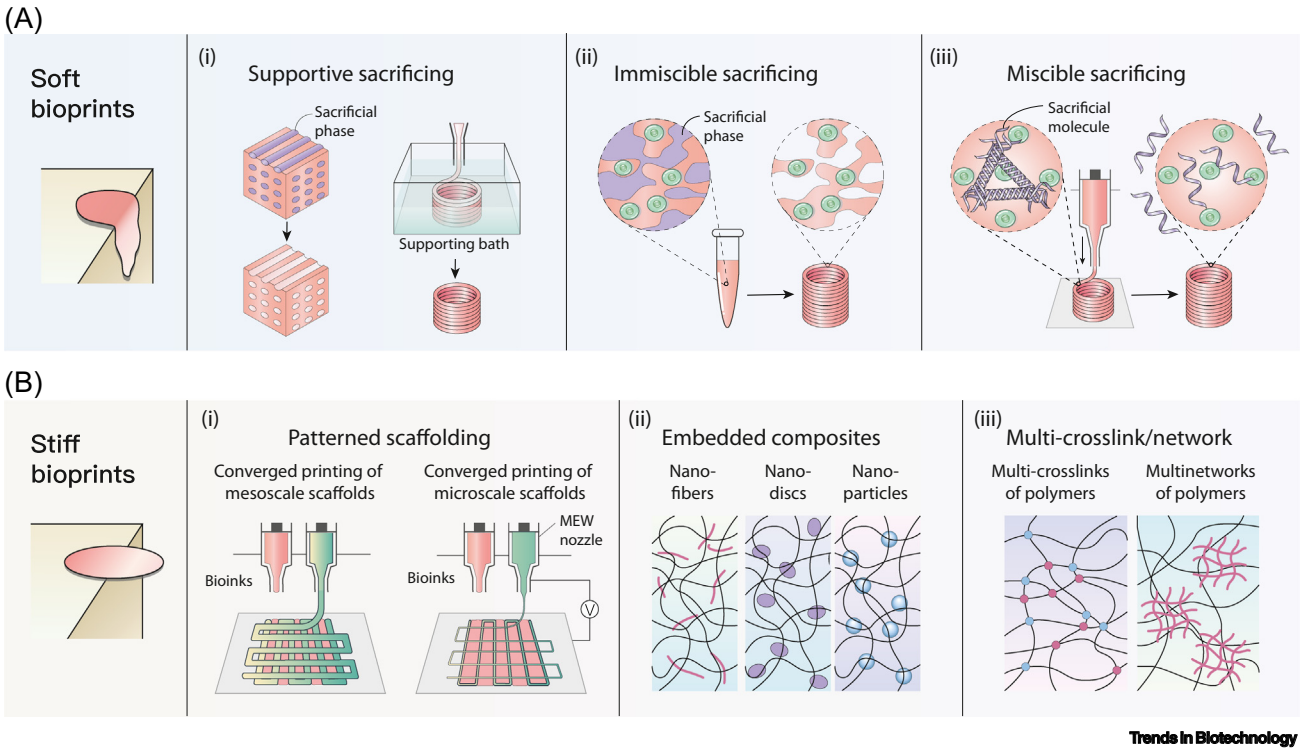

Figure 3. Representative strategies for pushing the mechanical boundaries of bioprints. (A) For the printing of soft constructs, sacrificial phases of varied forms are incorporated. (i) Macro or mesoscale sacrificial supporting could be applied via simultaneous printing with bioinks or suspension bioprinting. (ii) Immiscible sacrificial phases could also be directly incorporated in the bioink to temporarily shape the structure. (iii) Miscible sacrificial components in the bioink could template the construct at the molecular level. (B) For the printing of stiff constructs, different forms of mechanical reinforcement could be applied. (i) Patterned scaffolding combines acellular meso- or micro-scale frameworks with cellularized bioinks to provide strength (in the order of megapascal in modulus). (ii) Embedded nanocomposites are used to reinforce the soft hydrogels with the addition of nanofibers, nanodiscs, and nanoparticles. (iii) Another reinforcement strategy is to apply multi-crosslinking or a multinetwork to the hydrogels. Abbreviation: MEW, melt electrowriting.

collagen in a carbomer microgel bath, where cells were observed to infiltrate into the printed collagen and displayed extended morphology. However, the bioprints must be strong enough to bear the intrinsic energy of the surrounding bath.

An alternative approach is to introduce a supportive sacrificial phase in the bioinks. Zhang and colleagues [46] developed an aqueous two-phase emulsion bioink system composed of immiscible cell-laden GelMA and polyethylene oxide (PEO), which allowed for the construction of 3D constructs [Figure 3A(ii)]. After photo-crosslinking GelMA and washing away PEO, a porous hydrogel was obtained [46]. In their recent study [47], the authors found that a porous hydrogel (50% volume fraction of PEO) exhibited a dramatically decreased Young's modulus (1 kPa) compared with its bulk GelMA counterpart (23 kPa). Furthermore, such porous flexible bioprints could exhibit interesting injectability and shape-memory properties under specific parameters, demonstrating their potential use in low-invasive therapy scenarios. This approach relies on the unique pair of immiscible aqueous components, and the generalization to more hydrogels beyond GelMA needs to be investigated. In other studies [48], prefabricated sacrificial microgels were embedded in bioinks to temporarily support shape fidelity and template porosity. It should be noted that the connectivity of pores strongly depends on the initial volume fraction of the prefabricated microgels.

Another promising approach is to incorporate miscible sacrificial components into bioink formulations, with alginate [26] and gelatin [16,49] as representative sacrificial biomaterials. For example,

Zhang and colleagues [26] developed biomacromolecular bioinks templated by alginate. The addition of alginate (2 wt%) to the biomacromolecular solution aided the coaxial extrusion bioprinting process owing to the fast gelation of alginate with Ca^{2+}. After washing, more than 50% alginate was removed from the bioprints on day 3. More recently, soft cell-laden constructs have been printed in a highly generalizable manner by introducing a fixed amount of gelatin (5 wt%) to a library of photocrosslinking biomaterials, including gelatin, hyaluronic acid, dextran, chondroitin sulfate, alginate, heparin, and PEG [16] [Figure 3A(iii)]. The thermo-gelation properties introduced by gelatin allow for a standardized temperature-controlled bioprinting process with excellent printability. Meanwhile, the thermodissociation behavior of gelatin minimizes the polymer density and stiffness in the final bioprints (>80% gelatin was released on day 3 without intended washing steps). This approach could be readily used to fabricate methacrylated hyaluronic acid constructs with only a 0.5 wt% concentration (compression modulus 1–2 kPa), which is too soft to self-stand in the air but could retain its geometry when submerged in a buffer or culture medium. The successful bioprinting of 2.5 wt% GelMA with primary astrocytes also demonstrated the potential of soft bioprints in neural tissue engineering [16].

Bioprinting stiff constructs: mechanical reinforcement

A straightforward approach to enhance the mechanical properties of hydrogels is to incorporate an acellular polymeric framework. Although this can be achieved by infusing premade porous polymer scaffolds with cell-laden hydrogels, the so-called casting approach limits the freedom of using multiple materials/cells and customizing scaffold design. Cho and colleagues [50] used a multinozzle printer to print a polycaprolactone framework together with cell-laden **decellularized ECM** [Figure 3B(i)]. Such a hybrid construct was shown to be stable for 2 weeks with high cell viability and stem cell differentiation into tissue-specific lineages. Using a similar methodology, Atala and colleagues [51] developed an integrated tissue-organ printer to fabricate polycaprolactone framework-reinforced tissue constructs for calvarial bone, cartilage, and skeletal muscle engineering. This approach would yield an increase in the modulus from kilopascal to megapascal for the integrated construct, which is strongly dependent on the acellular polymetric scaffold [52,53]. These examples mainly involve the use of conventional extrusion techniques to deposit both acellular and cellularized parts with extruded fibers that are hundreds of micrometers in diameter. More recently, Castilho and colleagues [54] reported the simultaneous patterning of microfibrous meshes and cell-laden bioinks in a single-step fabrication process, where they combined **melt electrowriting** and extrusion bioprinting [Figure 3B(i)]. The patterned framework fibers possessed an average diameter of 13 μm. The compressive peak modulus increased from 19.85 ± 7.51 kPa to 246.84 ± 66.42 kPa using this fiber-reinforcement approach. No significant differences were observed in cell viability, metabolic activity, and cartilage-like matrix production between cast and converged printing, suggesting that the converged printing process could be optimized to minimize the side effects on cells.

Fiber reinforcement can also be achieved by embedding nanoscale fibers in bioinks [Figure 3B(ii)]. Gatenholm and colleagues [55] found that the addition of cellulose nanofibers to the alginate bioink improved the printability and reinforced the structural mechanics (~200 kPa of compressive modulus when the cellulose nanofibers-to-alginate ratio was 7:3). In addition to mechanical reinforcement, the addition of polylactic acid nanofibers into alginate bioinks was reported to allow for higher levels of cell proliferation and metabolic activity of human adipose-derived stem cells [56]. Electrically conductive nanomaterials have also been used to introduce additional functionalities. For example, carbon nanotubes have been added to bioinks to achieve electrically conductive nano-reinforcement for myocardial tissue regeneration [57]. Reduced graphene oxide was used to reinforce GelMA bioink (3 mg ml^{-1}) from 2 to 23 kPa for cardiac tissue engineering, with improved cardiac beating and contractility of seeded cardiomyocytes [58]. Other nanocomposites include disc- and dot-shaped nanomaterials [Figure 3B(ii)], such as

nesosilicates [59,60] and silica nanoparticles [55]. A study found that the inclusion of cationic silica nanoparticles increases the compressive modulus of hydrogel, while unmodified silica nanoparticles had limited effects, suggesting that electrostatic interaction might be an important mechanism for reinforcement [61]. Strain hardening can also be achieved by aligning nanomaterials during extrusion, with fibrous nanomaterials as a representative example. Despite the progress, the biocompatibility and safety of nanomaterials remains an issue for nanocomposite bioinks, as in other nanomaterial medical applications [62].

Another strategy for developing mechanically reinforced bioinks is the incorporation of multiple networks or crosslinks into the bioinks [Figure 3B(iii)]. A typical example is the development of bioinks composed of double networks with one interpenetrating into another for load sharing. Zhao and colleagues [63] employed a dual crosslinking mechanism to print a tough and stretchable hydrogel based on alginate and PEG. Alginate is ionically crosslinked using calcium ions, and PEG is covalently crosslinked using ultraviolet light. The resulting hydrogel was even tougher than the natural cartilage, which stretched three times its original length with fracture energy of 1500 J m^{-2}. Surprisingly, the viability of human embryonic kidney cells in these hydrogels was more than 75% over 7 days of culture. In another example [64], physically crosslinked gellan gum and chemically crosslinked PEG were combined to form a **double network hydrogel** bioink to strengthen the final constructs. The printed cell-laden construct possessed a Young's modulus of 184 kPa after a culture period of 21 days. Alternatively, multiple crosslinks can be incorporated into a single polymer. Supramolecular modification is a promising strategy for introducing desirable rheological properties for extrusion and mechanical reinforcement [65]. Various biopolymers can also be modified with functional side groups to allow for additional crosslinking mechanisms, in addition to the original one; these include the methacrylation of collagen and decellularized ECM for the introduction of photocrosslinking [66,67]. Through a special fabrication process, such as ionic reinforcement, the modulus of the printed hydrogel could reach the megapascal range (e.g., 40 MPa with chitosan), but the feasibility of cell printing warrants further research [68].

Concluding remarks and future perspectives

Expanding bioprinting windows to ease physical chemistry–biology trade-offs

Pushing the boundaries of typical material properties has significantly contributed toward the expansion of bioprinting windows, with representative examples shown in Table 1. The rationale

Table 1. Representative strategies for the expansion of bioprinting windows and corresponding examples

Bioprinting windows	Window boundaries	Representative strategies	Representative features of material properties	Example Refs
Rheology of bioinks	Liquid-like bioinks	*In situ* crosslinking Post-crosslinking Suspension bioprinting	η[a]: <15 mPa s G′: 1–2 Pa G′: <1 Pa	[20] [27] [32]
	Solid-like bioinks	Pre-crosslinking Granular microgels Entangled microstrands	G′: ~20 Pa G′: ~1000 Pa G′: ~1000 Pa	[33] [4] [5]
Mechanics of bioprints	Soft bioprints	Supportive sacrificing Immiscible sacrificing Miscible sacrificing	1.9 mg ml^{-1} collagen E[b]: 1 kPa 0.5 wt% MeHA[c], E: 1–2 kPa	[45] [47] [16]
	Stiff bioprints	Patterned scaffolding Embedded composites Multi-crosslink/network	E: ~MPa E: ~200 kPa E: ~200 kPa	[52] [60] [64]

[a] η: viscosity
[b] E: Young's modulus
[c] MeHA: methacrylated hyaluronic acid

Outstanding questions

Is there a universal strategy for harnessing the bioprinting process independent of bioink rheology?

How can printing resolution be maintained or even enhanced when expanding the windows of material properties?

How to match the mechanical properties of bioprints and matrices with the dynamic cellular process for the engineering of physiologically functional tissues?

How do the bioprinting windows apply to other bioprinting technologies?

What are the major obstacles to the translational application of 3D bioprinting, and what are the next steps?

behind this idea is to ease the trade-offs between the physicochemical and biological outcomes of 3D bioprinting. In this review, I define two sets of bioprinting windows with corresponding parameters, covering typical bioprinting and cultivation processes. For the bioprinting of liquid-like bioinks, the major principle is to maintain the structural shape postextrusion by applying appropriate crosslinking stimuli spatiotemporally. Regarding the bioprinting of solid-like bioinks, a primary focus would be to develop innovative forms of prefabricated gel bioinks that favor the printing process and, more importantly, protect viable cells. The basic methodology for printing super-soft constructs is to introduce a sacrificial phase, spanning a range of size scales from millimeters to nanometers. By contrast, the bioprinting of stiff constructs usually applies mechanical reinforcement mechanisms, from a microscaffolding framework to nanocomposite and molecular ingredients. I believe that the achievement of unusual material properties would significantly add to the capacity of bioprinting toward the engineering of more functional biological products. Apart from the rheological and mechanical properties, the biological properties of bioinks are vital for the bioprinting of functional tissues. Efforts have been made to engineer the bioinks with biofunctional peptides and growth factor-binding domains [69,70]. Despite these advances, there remain some critical questions (see Outstanding questions) to be answered.

Additional boundary toward cell-only or cell-rich bioinks: cells influence the rheology

The rheology of bioinks is very often discussed in terms of the properties of hydrogel biomaterials. However, the embedded cells would also affect rheology depending on the cell concentration [8,71]. For example, the addition of cells in collagen bioinks (cell concentration of 1×10^8 cells ml^{-1}) resulted in an increase and decrease in the storage modulus before and after gelation, respectively [72]. As biomaterials are not mandatory in a bioink [73] and native tissues exhibit a cell density of 10^8 per ml or higher, I envision a special category of bioinks toward cell-only or cell-rich formulations. Recently, Alsberg and colleagues [74] used human mesenchymal stem cell pellets as a bioink and directly printed them into a supporting bath composed of alginate microgels. The microgels not only serve as the temporal support for the bioprinting process but also hold the assembled human mesenchymal stem cell constructs for long-term culture (4 weeks). Feinberg and colleagues [31] also demonstrated the fabrication of a highly packed cell pellet using the suspension printing technique. They deposited cells (3×10^8 cardiomyocytes ml^{-1}) between printed collagen walls to form a human cardiac ventricle model, which performed impressive cardiac function. Without a sufficient crosslinkable matrix present in the bioink, it is unlikely to directly print cell-only or cell-rich formulations into self-standable constructs. The aspiration-based manipulation of cell spheroids has been used to print 3D material-free constructs [75]; however, proper fusion between spheroids is still needed before culturing without support. Nevertheless, it is still highly attractive to be able to print cell-only or cell-rich bioinks for the biofabrication of tissue constructs with tissue-relevant cell densities. The major challenges include (1) the availability of a large number of cells, (2) understanding the fundamental mechanisms of printing cell-rich bioinks, and (3) cell activity maintenance and vascularization in densely cellularized constructs.

Additional boundary toward mechanically dynamic bioprints

Tissue formation and maturation is a highly dynamic process in which cells interact with ECMs. It is naturally expected that time- and strain-dependent mechanical responses of engineered ECMs will mediate cell–matrix interactions. Recent progress in mechanobiology has also highlighted that the dynamic viscoelasticity of ECMs significantly influences cellular behavior, sometimes beyond our understanding of mechanotransduction based on an elastic matrix [18,76]. For example, Gerecht and colleagues [77] found that dynamic hydrogels based on imine and acylhydrazone bones increased the contractility of human endothelial colony-forming cells and promoted focal adhesion kinase and metalloproteinase expression, leading to the robust assembly of vasculatures surpassing that of their nondynamic counterparts. In the context of bioprinting,

I envision an additional boundary for mechanically dynamic bioprinted constructs in favor of cell behavior and tissue development. Some studies have introduced dynamic hydrogels to the bioprinting community, such as those based on supramolecular chemistry and dynamic covalent bonds [78]. Despite such considerable progress, further investigations are needed to couple the dynamic mechanics of bioprints and dynamic biological processes. Together, the field of bioprinting should progress from shape to biological function [79], which relies significantly on the 3D multiscale environment provided for cells, covering the biophysical, biochemical, and biological aspects.

Acknowledgments

The author acknowledges the funding from the National Natural Science Foundation of China (No. 52105306), New Faculty Start-up Funding provided by Tsinghua University (012 -53330200421), the discussion with Wei Sun and the reference collection assistance from Zixuan Wang, Yuzhi Guo, Chuqian Wang, Dezhi Zhou, and Runze Xu, all from the Department of Mechanical Engineering at Tsinghua University. The author acknowledges Li Li, an independent designer, for the production of figures.

Declaration of interests

No interests are declared.

References

1. Daly, A.C. *et al.* (2021) Bioprinting for the biologist. *Cell* 184, 18–32
2. Malda, J. *et al.* (2013) 25th anniversary article: engineering hydrogels for biofabrication. *Adv. Mater.* 25, 5011–5028
3. Schwab, A. *et al.* (2020) Printability and shape fidelity of bioinks in 3D bioprinting. *Chem. Rev.* 120, 11028–11055
4. Highley, C.B. *et al.* (2019) Jammed microgel inks for 3D printing applications. *Adv. Sci. (Weinh.)* 6, 1801076
5. Kessel, B. *et al.* (2020) 3D bioprinting of macroporous materials based on entangled hydrogel microstrands. *Adv. Sci. (Weinh.)* 7, 2001419
6. Pedde, R.D. *et al.* (2017) Emerging biofabrication strategies for engineering complex tissue constructs. *Adv. Mater.* 29, e1606061
7. Chimene, D. *et al.* (2020) Hydrogel bioink reinforcement for additive manufacturing: a focused review of emerging strategies. *Adv. Mater.* 32, e1902026
8. Ouyang, L. *et al.* (2016) Effect of bioink properties on printability and cell viability for 3D bioplotting of embryonic stem cells. *Biofabrication* 8, 035020
9. Lee, S.C. *et al.* (2020) Physical and chemical factors influencing the printability of hydrogel-based extrusion bioinks. *Chem. Rev.* 120, 10834–10886
10. Paxton, N. *et al.* (2017) Proposal to assess printability of bioinks for extrusion-based bioprinting and evaluation of rheological properties governing bioprintability. *Biofabrication* 9, 044107
11. Blaeser, A. *et al.* (2016) Controlling shear stress in 3D bioprinting is a key factor to balance printing resolution and stem cell integrity. *Adv. Healthc. Mater.* 5, 326–333
12. Nair, K. *et al.* (2009) Characterization of cell viability during bioprinting processes. *Biotechnol. J.* 4, 1168–1177
13. Ning, L. *et al.* (2018) Characterization of cell damage and proliferative ability during and after bioprinting. *ACS Biomater. Sci. Eng.* 4, 3906–3918
14. Soliman, B.G. *et al.* (2021) Development and characterization of gelatin-norbornene bioink to understand the interplay between physical architecture and micro-capillary formation in biofabricated vascularized constructs. *Adv. Healthc. Mater.* 2021, e2101873
15. Ouyang, L. *et al.* (2015) 3D printing of HEK 293FT cell-laden hydrogel into macroporous constructs with high cell viability and normal biological functions. *Biofabrication* 7, 015010
16. Ouyang, L. *et al.* (2020) Expanding and optimizing 3D bioprinting capabilities using complementary network bioinks. *Sci. Adv.* 6, eabc5529
17. Guimarães, C.F. *et al.* (2020) The stiffness of living tissues and its implications for tissue engineering. *Nat. Rev. Mater.* 5, 351–370
18. Chaudhuri, O. *et al.* (2020) Effects of extracellular matrix viscoelasticity on cellular behaviour. *Nature* 584, 535–546
19. Zhang, J. *et al.* (2020) Optimization of mechanical stiffness and cell density of 3D bioprinted cell-laden scaffolds improves extracellular matrix mineralization and cellular organization for bone tissue engineering. *Acta Biomater.* 114, 307–322
20. Ouyang, L. *et al.* (2017) A generalizable strategy for the 3D bioprinting of hydrogels from nonviscous photo-crosslinkable inks. *Adv. Mater.* 29, 1604983
21. Shao, L. *et al.* (2021) Pre-shear bioprinting of highly oriented porous hydrogel microfibers to construct anisotropic tissues. *Biomater. Sci.* 9, 6763–6771
22. Mirani, B. *et al.* (2021) Microfluidic 3D printing of a photo-cross-linkable bioink using insights from computational modeling. *ACS Biomater. Sci. Eng.* 7, 3269–3280
23. Hwangbo, H. *et al.* (2022) Bio-printing of aligned GelMa-based cell-laden structure for muscle tissue regeneration. *Bioact. Mater.* 8, 57–70
24. Soliman, B.G. *et al.* (2020) Stepwise control of crosslinking in a one-pot system for bioprinting of low-density bioinks. *Adv. Healthc. Mater.* 9, e1901544
25. Colosi, C. *et al.* (2016) Microfluidic bioprinting of heterogeneous 3D tissue constructs using low-viscosity bioink. *Adv. Mater.* 28, 677–684
26. Zhu, K. *et al.* (2018) A general strategy for extrusion bioprinting of bio-macromolecular bioinks through alginate-templated dual-stage crosslinking. *Macromol. Biosci.* 18, e1800127
27. Ning, L. *et al.* (2019) Bioprinting Schwann cell-laden scaffolds from low-viscosity hydrogel compositions. *J. Mater. Chem. B* 7, 4538–4551
28. Gao, Q. *et al.* (2015) Coaxial nozzle-assisted 3D bioprinting with built-in microchannels for nutrients delivery. *Biomaterials* 61, 203–215
29. Kim, H. *et al.* (2021) Light-activated decellularized extracellular matrix-based bioinks for volumetric tissue analogs at the centimeter scale. *Adv. Funct. Mater.* 31, e2011252
30. McCormack, A. *et al.* (2020) 3D printing in suspension baths: keeping the promises of bioprinting afloat. *Trends Biotechnol.* 38, 584–593
31. Lee, A. *et al.* (2019) 3D bioprinting of collagen to rebuild components of the human heart. *Science* 365, 482–487
32. Hinton, T.J. *et al.* (2015) Three-dimensional printing of complex biological structures by freeform reversible embedding of suspended hydrogels. *Sci. Adv.* 1, e1500758
33. Dubbin, K. *et al.* (2016) Dual-stage crosslinking of a gel-phase bioink improves cell viability and homogeneity for 3D bioprinting. *Adv. Healthc. Mater.* 5, 2488–2492
34. Jeon, O. *et al.* (2019) Cryopreserved cell-laden alginate microgel bioink for 3D bioprinting of living tissues. *Mater. Today Chem.* 12, 61–70

35. Song, K. *et al.* (2020) Injectable gelatin microgel-based composite ink for 3D bioprinting in air. *ACS Appl. Mater. Interfaces* 12, 22453–22466
36. Xin, S. *et al.* (2019) Clickable PEG hydrogel microspheres as building blocks for 3D bioprinting. *Biomater. Sci.* 7, 1179–1187
37. Song, K. *et al.* (2021) Computational study of extrusion bioprinting with jammed gelatin microgel-based composite ink. *Addit. Manuf.* 41, 101963
38. Xin, S. *et al.* (2021) Generalizing hydrogel microparticles into a new class of bioinks for extrusion bioprinting. *Sci. Adv.* 7, eabk3087
39. Seymour, A.J. *et al.* (2021) 3D printing of microgel scaffolds with tunable void fraction to promote cell infiltration. *Adv. Healthc. Mater.* 10, e2100644
40. Tan, Z. *et al.* (2017) Cryogenic 3D printing of super soft hydrogels. *Sci. Rep.* 7, 16293
41. Naghieh, S. *et al.* (2019) Indirect 3D bioprinting and characterization of alginate scaffolds for potential nerve tissue engineering applications. *J. Mech. Behav. Biomed. Mater.* 93, 183–193
42. Cui, X. *et al.* (2020) Rapid photocrosslinking of silk hydrogels with high cell density and enhanced shape fidelity. *Adv. Healthc. Mater.* 9, e1901667
43. Ouyang, L. *et al.* (2020) Void-free 3D bioprinting for *in-situ* endothelialization and microfluidic perfusion. *Adv. Funct. Mater.* 30, 1908349
44. Noor, N. *et al.* (2019) 3D printing of personalized thick and perfusable cardiac patches and hearts. *Adv. Sci. (Weinh.)* 6, 1900344
45. Zhang, Y. *et al.* (2021) 3D printed collagen structures at low concentrations supported by jammed microgels. *Bioprinting* 21, e00121
46. Ying, G.L. *et al.* (2018) Aqueous two-phase emulsion bioink-enabled 3D bioprinting of porous hydrogels. *Adv. Mater.* 30, e1805460
47. Ying, G. *et al.* (2020) Bioprinted injectable hierarchically porous gelatin methacryloyl hydrogel constructs with shape-memory properties. *Adv. Funct. Mater.* 30, 2003740
48. Shao, L. *et al.* (2020) Sacrificial microgel-laden bioink-enabled 3D bioprinting of mesoscale pore networks. *Bio Design Manuf.* 3, 30–39
49. Yin, J. *et al.* (2018) 3D bioprinting of low-concentration cell-laden gelatin methacrylate (GelMA) bioinks with a two-step cross-linking strategy. *ACS Appl. Mater. Interfaces* 10, 6849–6857
50. Pati, F. *et al.* (2014) Printing three-dimensional tissue analogues with decellularized extracellular matrix bioink. *Nat. Commun.* 5, 3935
51. Kang, H.W. *et al.* (2016) A 3D bioprinting system to produce human-scale tissue constructs with structural integrity. *Nat. Biotechnol.* 34, 312–319
52. Daly, A.C. *et al.* (2016) A comparison of different bioinks for 3D bioprinting of fibrocartilage and hyaline cartilage. *Biofabrication* 8, 045002
53. Critchley, S. *et al.* (2020) 3D printing of fibre-reinforced cartilaginous templates for the regeneration of osteochondral defects. *Acta Biomater.* 113, 130–143
54. de Ruijter, M. *et al.* (2019) Simultaneous micropatterning of fibrous meshes and bioinks for the fabrication of living tissue constructs. *Adv. Healthc. Mater.* 8, e1800418
55. Markstedt, K. *et al.* (2015) 3D bioprinting human chondrocytes with nanocellulose-alginate bioink for cartilage tissue engineering applications. *Biomacromolecules* 16, 1489–1496
56. Narayanan, L.K. *et al.* (2016) 3D-bioprinting of polylactic acid (PLA) nanofiber-alginate hydrogel bioink containing human adipose-derived stem cells. *ACS Biomater. Sci. Eng.* 2, 1732–1742
57. Izadifar, M. *et al.* (2018) UV-Assisted 3D bioprinting of nanoreinforced hybrid cardiac patch for myocardial tissue engineering. *Tissue Eng. C Methods* 24, 74–88
58. Shin, S.R. *et al.* (2016) Reduced graphene oxide-GelMA hybrid hydrogels as scaffolds for cardiac tissue engineering. *Small* 12, 3677–3689
59. Nadernezhad, A. *et al.* (2019) Nanocomposite bioinks based on agarose and 2D nanosilicates with tunable flow properties and bioactivity for 3D bioprinting. *ACS Appl. Bio. Mater.* 2, 796–806
60. Wilson, S.A. *et al.* (2017) Shear-thinning and thermo-reversible nanoengineered inks for 3D bioprinting. *ACS Appl. Mater. Interfaces* 9, 43449–43458
61. Lee, M. *et al.* (2018) Exploitation of cationic silica nanoparticles for bioprinting of large-scale constructs with high printing fidelity. *ACS Appl. Mater. Interfaces* 10, 37820–37828
62. Hajiali, H. *et al.* (2021) Review of emerging nanotechnology in bone regeneration: progress, challenges, and perspectives. *Nanoscale* 13, 10266–10280
63. Hong, S. *et al.* (2015) 3D printing of highly stretchable and tough hydrogels into complex, cellularized structures. *Adv. Mater.* 27, 4035–4040
64. Wu, D. *et al.* (2018) 3D bioprinting of gellan gum and poly (ethylene glycol) diacrylate based hydrogels to produce human-scale constructs with high-fidelity. *Mater. Des.* 160, 486–495
65. Ouyang, L. *et al.* (2016) 3D printing of shear-thinning hyaluronic acid hydrogels with secondary cross-linking. *ACS Biomater. Sci. Eng.* 2, 1743–1751
66. Visscher, D.O. *et al.* (2021) A photo-crosslinkable cartilage-derived extracellular matrix bioink for auricular cartilage tissue engineering. *Acta Biomater.* 121, 193–203
67. Tytgat, L. *et al.* (2020) High-resolution 3D bioprinting of photo-cross-linkable recombinant collagen to serve tissue engineering applications. *Biomacromolecules* 21, 3997–4007
68. Wang, X. *et al.* (2018) Fabrication of multiple-layered hydrogel scaffolds with elaborate structure and good mechanical properties via 3D printing and ionic reinforcement. *ACS Appl. Mater. Interfaces* 10, 18338–18350
69. Hedegaard, C.L. *et al.* (2018) Hydrodynamically guided hierarchical self-assembly of peptide-protein bioinks. *Adv. Funct. Mater.* 28, 1703716
70. Wang, B. *et al.* (2021) Affinity-bound growth factor within sulfated interpenetrating network bioinks for bioprinting cartilaginous tissues. *Acta Biomater.* 128, 130–142
71. Distler, T. *et al.* (2021) Mechanical properties of cell- and microgel bead-laden oxidized alginate-gelatin hydrogels. *Biomater. Sci.* 9, 3051–3068
72. Diamantides, N. *et al.* (2019) High density cell seeding affects the rheology and printability of collagen bioinks. *Biofabrication* 11, 045016
73. Groll, J. *et al.* (2018) A definition of bioinks and their distinction from biomaterial inks. *Biofabrication* 11, 013001
74. Jeon, O. *et al.* (2019) Individual cell-only bioink and photocurable supporting medium for 3D printing and generation of engineered tissues with complex geometries. *Mater. Horiz.* 6, 1625–1631
75. Ayan, B. *et al.* (2020) Aspiration-assisted bioprinting for precise positioning of biologics. *Sci. Adv.* 6, eaaw5111
76. Tang, S. *et al.* (2021) Dynamic covalent hydrogels as biomaterials to mimic the viscoelasticity of soft tissues. *Prog. Mater. Sci.* 120, 100738
77. Wei, Z. *et al.* (2020) Hydrogel network dynamics regulate vascular morphogenesis. *Cell Stem Cell* 27, 798–812.e796
78. Morgan, F.L.C. *et al.* (2020) Dynamic bioinks to advance bioprinting. *Adv. Healthc. Mater.* 9, e1901798
79. Levato, R. *et al.* (2020) From shape to function: the next step in bioprinting. *Adv. Mater.* 32, e1906423
80. Fu, Z. *et al.* (2022) Responsive biomaterials for 3D bioprinting: a review. *Mater. Today* https://doi.org/10.1016/j.mattod.2022.01.001